Supplementary information

Measuring ligand binding kinetics to membrane proteins using virion nano-oscillators

Guangzhong Ma*,[1] Guan-Da Syu*,[3,4,5] Xiaonan Shan,[1,2] Brandon Henson,[3] Shaopeng Wang,[1] Prashant J. Desai**,[3] Heng Zhu**,[4,5] Nongjian Tao**[1,2]

[1]Biodesign Center for Bioelectronics and Biosensors, Arizona State University, Tempe, AZ 85287, USA

[2]School of Electrical, Computer and Energy Engineering, Arizona State University, Tempe, AZ 85287

[3]Viral Oncology Program, The Sidney Kimmel Comprehensive Cancer Center at Johns Hopkins, Baltimore, MD 21231

[4]Department of Pharmacology and Molecular Sciences, Johns Hopkins School of Medicine, Baltimore, MD 21205

[5]Center for High-Throughput Biology, Johns Hopkins School of Medicine, Baltimore, MD 21205

*These authors contribute equally to the work.

**njtao@asu.edu; hzhu4@jhmi.edu; pdesai@jhmi.edu

Equation of motion of virion oscillators

The motion of a virion-oscillator under an electric field is described by,

$$m\frac{d^2z}{dt^2} + c\frac{dz}{dt} + kz = qE, \quad \text{(S1)}$$

where z, m, q, c, k, E are displacement, mass, charge of the virion, damping coefficient of the virion, spring constant of the linker, and electric field, respectively. Because the mass of virion is small, and the PEG linkers are soft, the first and the third terms of Eq. S1 are small compared to the damping term (second term), and Eq. S1 is simplified as

$$c\frac{dz}{dt} = 6\pi\eta a\frac{dz}{dt} = qE, \qquad \text{(S2)}$$

where η and a are viscosity of the solution and the radius of the virion. For a sinusoidal applied field, the electric field can be written as $E = E_0 e^{j\omega t}$ and the displacement of the oscillator is $z = z_0 e^{j\omega t}$, where ω is angular frequency and $\omega = 2\pi f$. By substituting z and E in Eq. S2, we obtain,

$$z_0 = \frac{qE_0}{j12\pi^2\eta f a}, \qquad \text{(S3)}$$

According to the Einstein relation (Eq. 3), Eq. S3 can be written as

$$z_0 = \frac{1}{j2\pi f} \cdot \frac{qD}{k_B T} \cdot E_0 = \frac{\mu}{j2\pi f} E_0, \qquad \text{(S4)}$$

where μ is the electrical mobility of the virion.

Binding-induced viscosity change

Ligand binding causes a change in the size and shape of the target protein, which could, in principle, change the viscosity of the virion. For the binding of small molecule ligands to the membrane proteins in the virion, the size change of the virion is expected to be less than 1 nm,[1] which is insignificant compared to the diameter of the virion (~160 nm), so the corresponding viscosity change should be relatively small[2-4]. The binding of large ligands (e.g., proteins), the size change can be 5-10 nm, leading to a larger viscosity change (50%) according to literature.[5, 6]

The viscosity of polymer can be estimated with Mark-Houwink relation, $[\boldsymbol{\eta}] = \boldsymbol{KM^{\alpha}}$, where $[\eta]$ is the intrinsic viscosity of the polymer, M is the molecular weight of the polymer, K is a parameter which depends on the polymer-solvent system, and α is a parameter related to the stiffness of the polymer. Here we use an empirical equation derived from Mark-Houwink relation to estimate the viscosity of protein,[7] where the viscosity is expressed as a function of the number of amino acid residues (n),

$$[\eta] = 0.732n^{0.656}. \quad \text{(S5)}$$

For GPCR - small molecule interaction, the initial n value for a GPCR molecule is ~350 and the binding of a small molecule introduces about 800 Da in mass, which corresponds to 7 amino acid residues. As a result, the viscosity change is 1%, which is much smaller than the charge change associated with molecular binding (see main text for details).

Surface charge fluctuation

The virion-oscillator detection technology can detect charge change as small as a couple electron charges (e). With this high charge sensitivity, intrinsic charge fluctuations associated with the binding/unbinding of ions and charged molecules on the virions become an important source of noise. To estimate this noise, we measured the oscillation amplitude of a virion-oscillator over one minute at 0.4 V (E~150 V/m) and 5 Hz (Figure S3). The mean value, and the standard deviation (noise) of the oscillation amplitude were determined to be 42.8 nm and 3.9 nm, which correspond to -253e and -23e charges after considering ionic screening effect (see discussion below). For a surface with N electron charges, the charge fluctuation is of the order of √N. Therefore, the estimated charge fluctuation for the virion-oscillator with charge -253e is ~15.9e, smaller than the measured charge fluctuation. Other sources of noise, such as the Brownian motion of the virion, mechanical vibration of the optical system, and virion-gold surface adhesion, could also contribute to the observed noise in the current setup.

Charge screening effect

The charge measured with the virion-oscillator should be regarded as an effective charge because of ionic screening. The charge screening effect can be estimated by

$$\frac{\sigma_{eff}}{\sigma_{total}} = \frac{\zeta}{\psi} = \exp(-\kappa x), \qquad \text{(S6)}$$

where σ_{eff} and σ_{total} are the effective and total surface charge density on the virion, ζ is zeta potential, ψ is the potential at the surface, x is the slipping layer thickness, and κ^{-1} is the Debye length. In 6 mM PBS solution, the Debye length is 4 nm, according to the Debye-Hückel equation,

$$\boldsymbol{\kappa^{-1}} = \sqrt{\frac{\varepsilon\varepsilon_0 k_B T}{2N_A e^2 c}}, \qquad \text{(S7)}$$

where $\boldsymbol{\varepsilon}$ is the dielectric constant of the solution, $\boldsymbol{\varepsilon_0}$ is the permittivity of the free space, $\boldsymbol{k_B}$ is the Boltzmann constant, $\boldsymbol{T}$ is temperature, $\boldsymbol{N_A}$ is the Avogadro number, and $\boldsymbol{c}$ is the ionic strength. From Eq. S6 we obtained the slipping layer thickness by measuring the zeta potentials of the 540 nm streptavidin coated silica beads at two different PBS concentrations

$$\boldsymbol{x} = \frac{\ln\frac{\zeta_1}{\zeta_2}}{\kappa_2 - \kappa_1}, \quad \text{(S8)}$$

For 3.5 mM PBS, $\boldsymbol{\zeta_1 = -36.2\ \mathrm{mV}}$, $\boldsymbol{\kappa_1 = 0.193\ \mathrm{nm^{-1}}}$, and for 15 mM PBS, $\boldsymbol{\zeta_2 = -16.0\ \mathrm{mV}}$, $\boldsymbol{\kappa_2 = 0.412}$, from which the slipping layer thickness is $\boldsymbol{x = 3.73\ \mathrm{nm}}$. The charge screening effect plotted vs. concentration in Figure S1. In 1xPBS, charge screening is substantial (Figure S1b). We use 4 mM PBS to reduce charge screening down to 54% (Figure S1b). When applying the virion-oscillator detection technology to study molecular binding kinetics, we should consider this ionic screening effect.

Heterogeneity in the virions

The heterogeneity in the virions (Figure 4) reflects variability in the size and membrane expression level of different virions. To confirm this, we measured the sizes of 148 individual virions from the plasmonic image intensities[8], and determined average diameter of 157 nm with a standard deviation of 15 nm (Figure S4). We also observed that the binding curves of some virions could not be fitted with the simple first order kinetic model (Figure S5), which may be attributed to incompletely assembled virions.[9]

Measuring binding-induced mobility changes in virions with electrophoretic light scattering (ELS)

To confirm the oscillation amplitude change was due to the binding-induced mobility change, we measured the mobility of virions before and after binding using ELS (Zetasizer Nano, Malvern Instruments). The mobility of DRD1, GPR55, and ADRB2 virions were measured in 40 times diluted PBS (concentration is ~10^7 virions/ml) before introducing the ligands, and the mobility were -(1.53±0.39)×10^{-8} $m^2/(V \cdot s)$, -(1.59±0.38)×10^{-8} $m^2/(V \cdot s)$, and –(1.52±0.37)×10^{-8} $m^2/(V \cdot s)$, respectively (Figure S6). Then DRD1, GPR55, and ADRB2 virions were mixed with 10 nM D1 antagonist, 100 nM Tocrifluor, and 100 nM B2 antagonist, respectively to allow binding of the ligands to the GPCRs on the virions. After incubation of the virions for 30 minutes to reach equilibrium, the mobility of the virions were measured again. As a result, all the three types of virions showed decreased mobility after binding with the ligands. The mobility of DRD1, GPR55, and ADRB2 virions were –(0.69±0.39)×10^{-8} $m^2/(V \cdot s)$, –(0.44±0.36)×10^{-8} $m^2/(V \cdot s)$, and –(0.76±0.42)×10^{-8} $m^2/(V \cdot s)$, respectively. The mobility (before and after binding) were consistent with those measured with virion-oscillators in both polarity and amplitude. We also performed a control experiment using K082, a virion that does not bind to any of the three ligands. As expected, none of the ligands induced mobility change in K082. This result confirms that the mobility changes of the virions were indeed induced by ligand binding.

Measuring dissociation constant (K_D) with fluorescence detection

Fluorescence detection is a method used for measuring the dissociation constant of ligand-receptor binding. The method is used here to measure the dissociation constants of DRD1 – D1 antagonist, GPR55 – Tocrifluor, and ADRB2 – B2 antagonist, and the results are consistent with those obtained with the virion-oscillators. To perform the measurement, the virions were first immobilized on a glass slide. Briefly, the glass slide was cleaned and salinized with (3-glycidyloxypropyl)trimethoxysilane, and then the virions were immobilized on the glass via epoxy-amine reaction. Then the small molecule ligand was introduced and incubated for 30 minutes to allow the binding to reach equilibrium. Finally, the slide was flushed with PBS to remove unbound ligands in the solution, and the fluorescence was measured immediately. We plotted the equilibrium fluorescence intensity vs. small molecule concentration in Figure S7, and K_D for DRD1-D1 antagonist, GPR55-Tocrifluor, and ADRB2-B2 antagonist were 7.5 ± 2.2 nM, 155 ± 45 nM, and 440 ± 48 nM, respectively, which were close to those measured by the virion-oscillators.

Virion oscillation model

During virion oscillation, the largest virion-gold chip distance (z) is determined by the length (63 nm) of the PEG10k linkers (Figure S9) and the smallest distance is determined by the hydrodynamic radius of PEG10k, which is reflected by the Flory radius,[10]

$$R_F = aN^{\nu}, \quad \text{(S9)}$$

where a is the length of monomer, N is the degree of polymerization, and ν is the Flory exponent and equals to 0.6 under high-solubility conditions[10]. For the PEG10k linker, a = 0.278 nm and N

= 225, therefore R_F = 7.17 nm. The smallest virion-gold chip distance should be $2R_F$, which is about 14 nm.

The plasmonic imaging intensity (I) of a virion can be determined by measuring the intensity change induced by the virion binding to the gold chip surface[8] (Figure S4). The plasmonic imaging intensity of an ADRB2 virion is 230 a.u. in intensity or 69 mDeg change in surface plasmon resonance angle. According to Eq.2, the intensity of the virion at z = 14 nm is 214 a.u. This value was used in the calculations (see data processing section below).

Data processing

A detailed data processing example is given in Figure S10, which shows the procedures for obtaining the kinetic constants of DRD1 – D1 antagonist interaction. In the experiment, the association process was initiated by injecting 200 nM D1 antagonist at the 80th second and the dissociation process was initiated by injecting buffer at the 280th second.

Step 1. The oscillation of virion-oscillators is recorded by the CCD camera during the binding experiment. The frame rate is 106.5 and 60175 images are recorded.

Step 2. The intensity of a virion region (I_v) and a reference region (I_r) are measured for every single image and plotted vs. time. The periodic intensity change reflects oscillation for the virion region and double layer charging for the reference region. The blue and the red shadows indicate the injection of buffer and small molecule, respectively. The inset shows the zoom-in of the section marked in red.

Step 3. The oscillation signal (I) of the virion is obtained by $I = I_v - I_r$.

Step 4. Using the model in Figure S9, we assume the maximum intensity in each oscillation cycle results from the virion approaches the smallest virion-gold chip surface distance, which is 14 nm. Accordingly, the oscillation signal (I) is processed by aligning the maximum intensity in each cycle to I = 214 a.u., where z = 14 nm.

Step 5. The aligned intensity is converted to virion-surface distance using Eq. 2.

Step 6. The oscillation amplitude in each second is obtained by performing FFT on the virion-surface distance. The pronounced peak at the applied frequency (5 Hz) is the oscillation amplitude.

Step 7. The oscillation amplitude is plotted vs. time. Because DRD1 virions are negatively charged and D1 antagonist is positively charged, the binding of D1 antagonist induces a decrease in oscillation amplitude.

Step 8. In order to fit the binding curve, the initial oscillation amplitude is set to be zero (baseline) and y-axis is re-expressed as the absolute value of the oscillation amplitude change. The curve is fitted to the first order kinetics model because one D1 antagonist molecule binds to one DRD1 molecule[11].

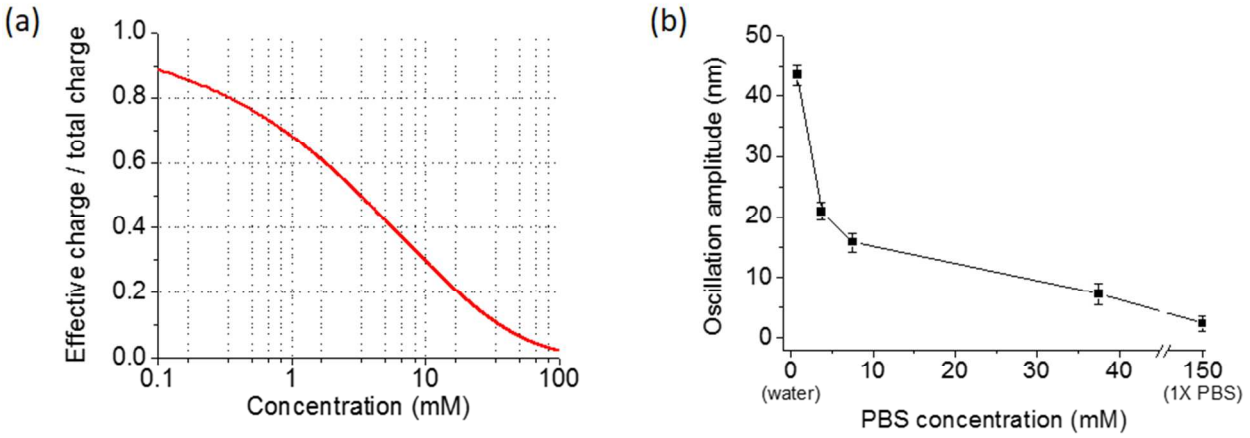

Figure S1. Evaluation of charge screening on virion-oscillator detection technology. (a) Effective charge of a charged in PBS buffers (of different concentrations). (b) Dependence of oscillation amplitude on PBS concentration. The voltage modulation amplitude: 0.2 V and frequency: 5 Hz.

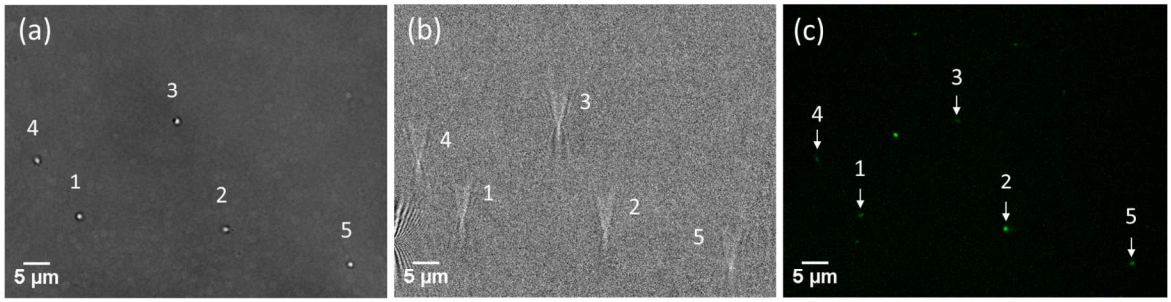

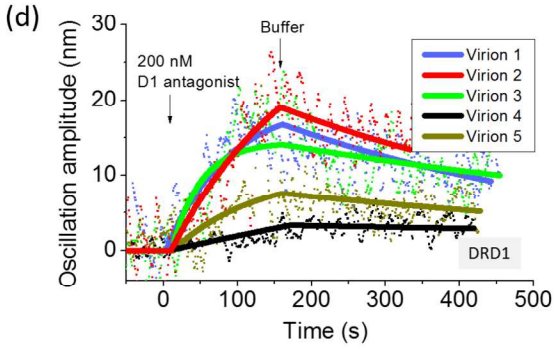

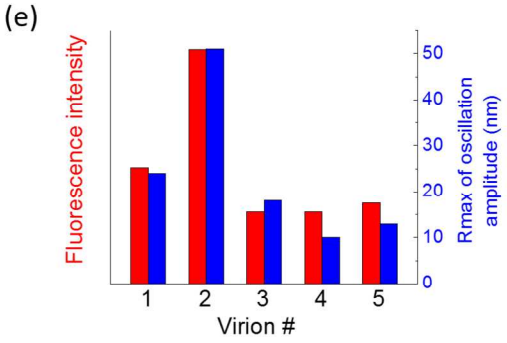

(f)

Virion #	k_a ($M^{-1}\cdot s^{-1}$)	k_d (s^{-1})	k_D (nM)
1	4.9×10^4	2.1×10^{-3}	43
2	1.8×10^4	2.0×10^{-3}	1.1×10^2
3	9.0×10^4	1.0×10^{-3}	11
4	8.1×10^3	5.7×10^{-4}	71
5	4.0×10^4	1.4×10^{-3}	35

Figure S2. Validation of small molecule binding measured by the virion-oscillator with fluorescence detection. Five virion-oscillators with DRD1 virions imaged by bright field (a), plasmonic (b) and fluorescence imaging (c) techniques. (d) Binding kinetic curves of DRD1-D1 antagonist interaction obtained from the amplitudes of the virion-oscillators, where the solid lines are fitting of the data to the first order kinetics. D1 antagonist concentration: 200 nM. (e) Correlation of fluorescence intensity with maximum response (Rmax) of oscillation amplitude. The fluorescence intensity was measured from the fluorescence images (e.g., c), and the Rmax values were from the fitting (e.g., d). (f) Kinetic and equilibrium constants of DRD1-D1 antagonist interaction obtained from the five individual virions.

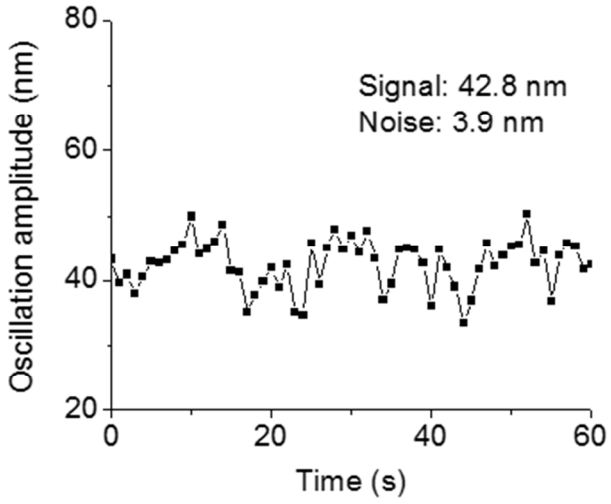

Figure S3. Oscillation amplitude of a virion-oscillator. The oscillation amplitude is 42.8 nm with a standard deviation of 3.9 nm.

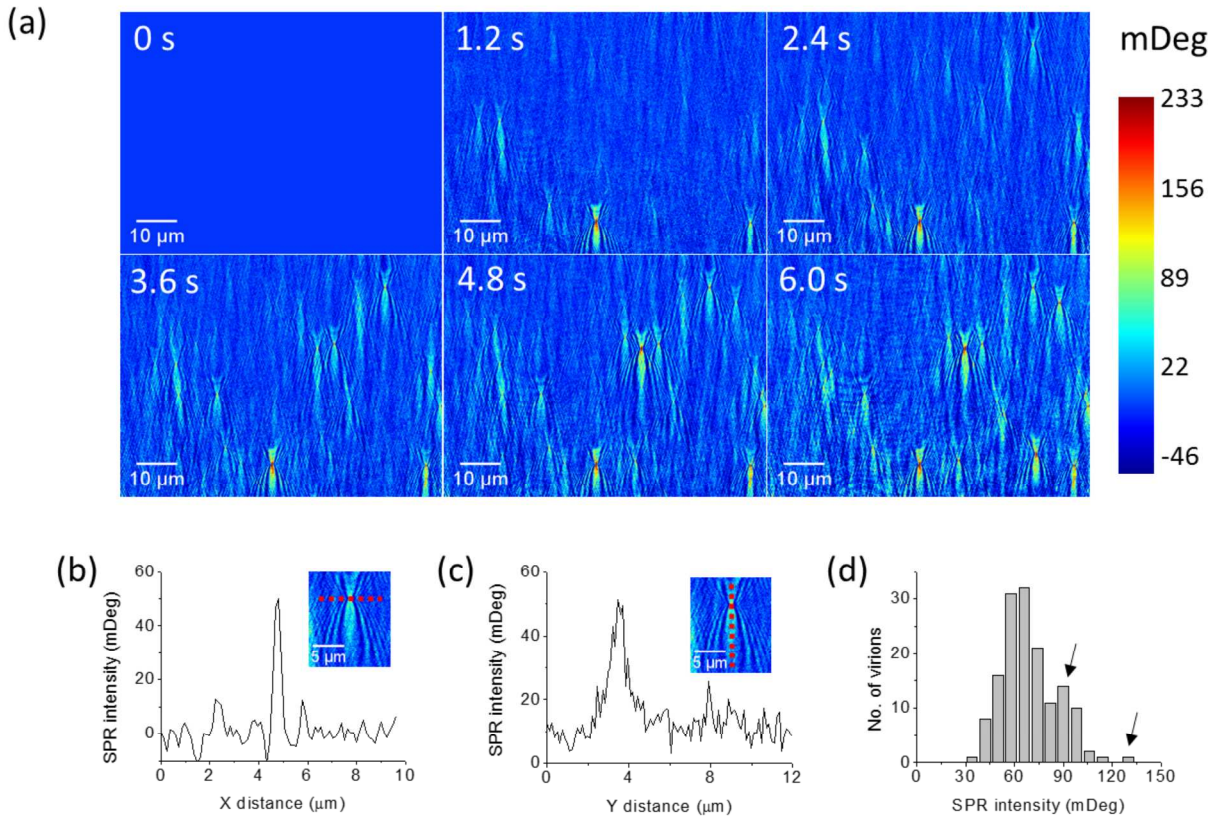

Figure S4. Measuring size distribution of the virions with plasmonic imaging. (a) Time sequence plasmonic images of gold surface in 10^4/μL ADRB2 virions. (b)-(c) Plasmonic image intensity profiles of a selected virion in x and y direction (marked by the dashed lines in the insets). (d) Plasmonic image intensity histogram of 148 individual virions, showing an averaged intensity of 69.2 ± 17.0 mDeg for a single virion, corresponding to 157.4 ± 14.8 nm in virion size (diameter). The peaks marked by arrows indicate the formation of dimers and trimers.

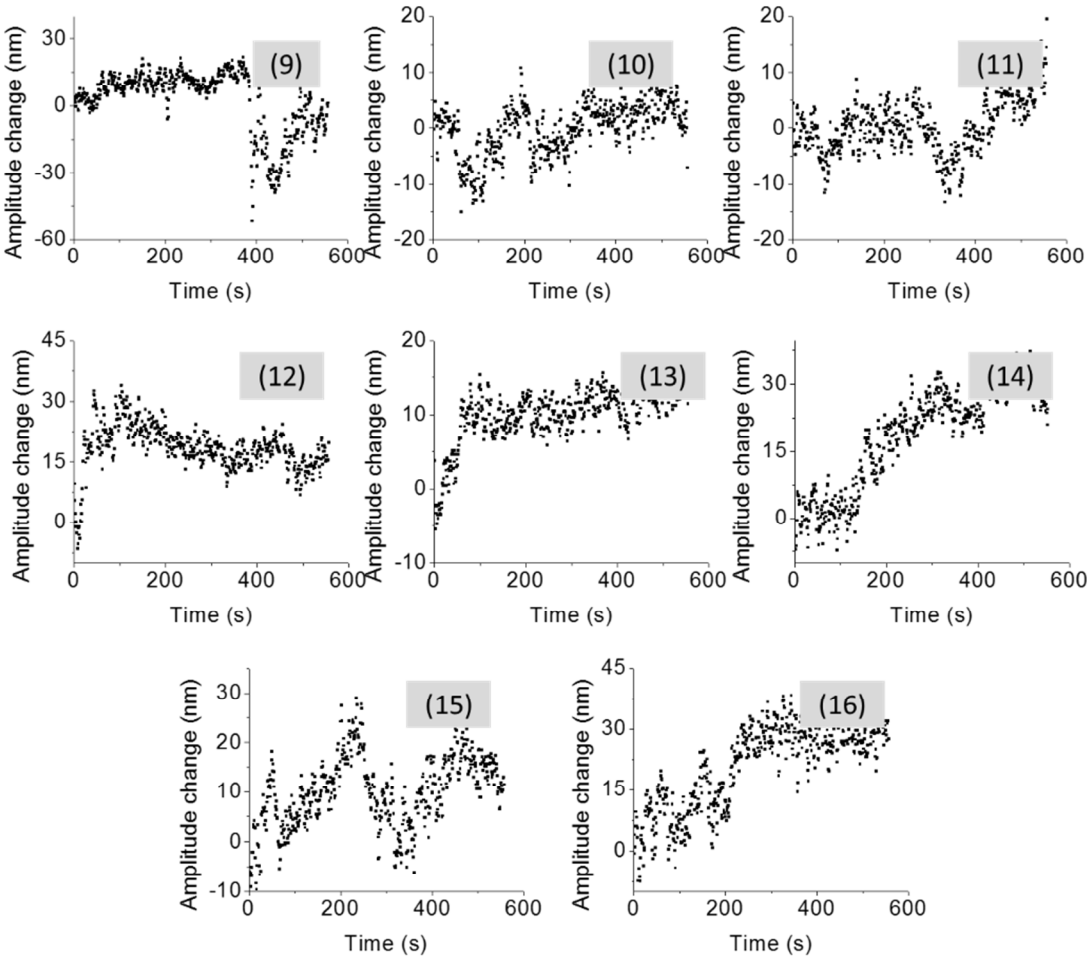

Figure S5. Tocrifluor-GPR55 binding curves from some of the virions labeled with numbers in Figure 4. The binding kinetic curves could not be fitted with simple kinetic models, which are attributed to incompletely assembled or broken virions (see main text for more details).

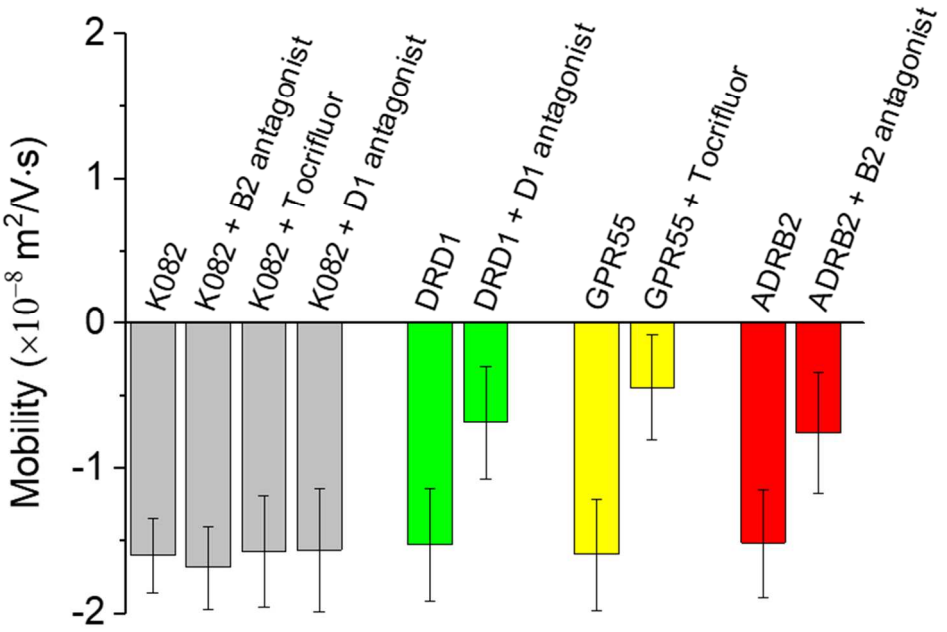

Figure S6. Measuring the mobility of virions and mobility changes induced by ligand binding with electrophoretic light scattering (ELS). The concentration of D1 antagonist, Tocrifluor, and B2 antagonist are 10 nM, 100 nM, and 100 nM, respectively. The buffer is 40 times diluted PBS with pH = 7.4.

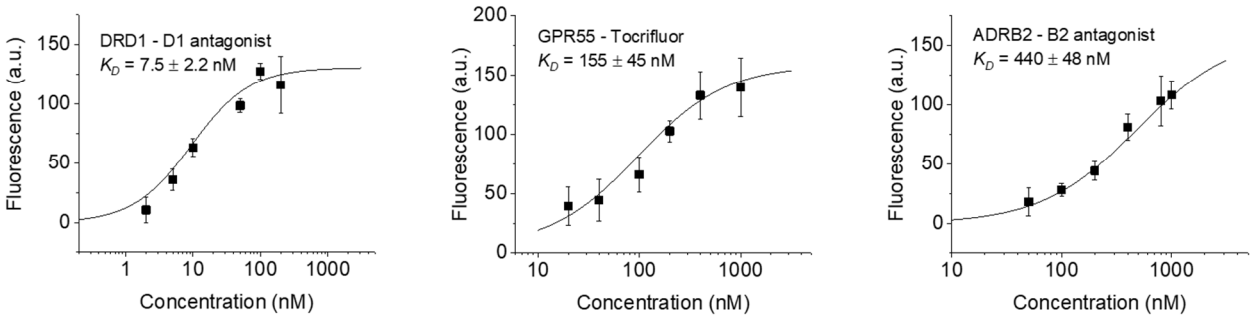

Figure S7. Measuring dissociation constant (K_D) with fluorescence detection. The data points and error bars are the mean values and the standard deviations, respectively.

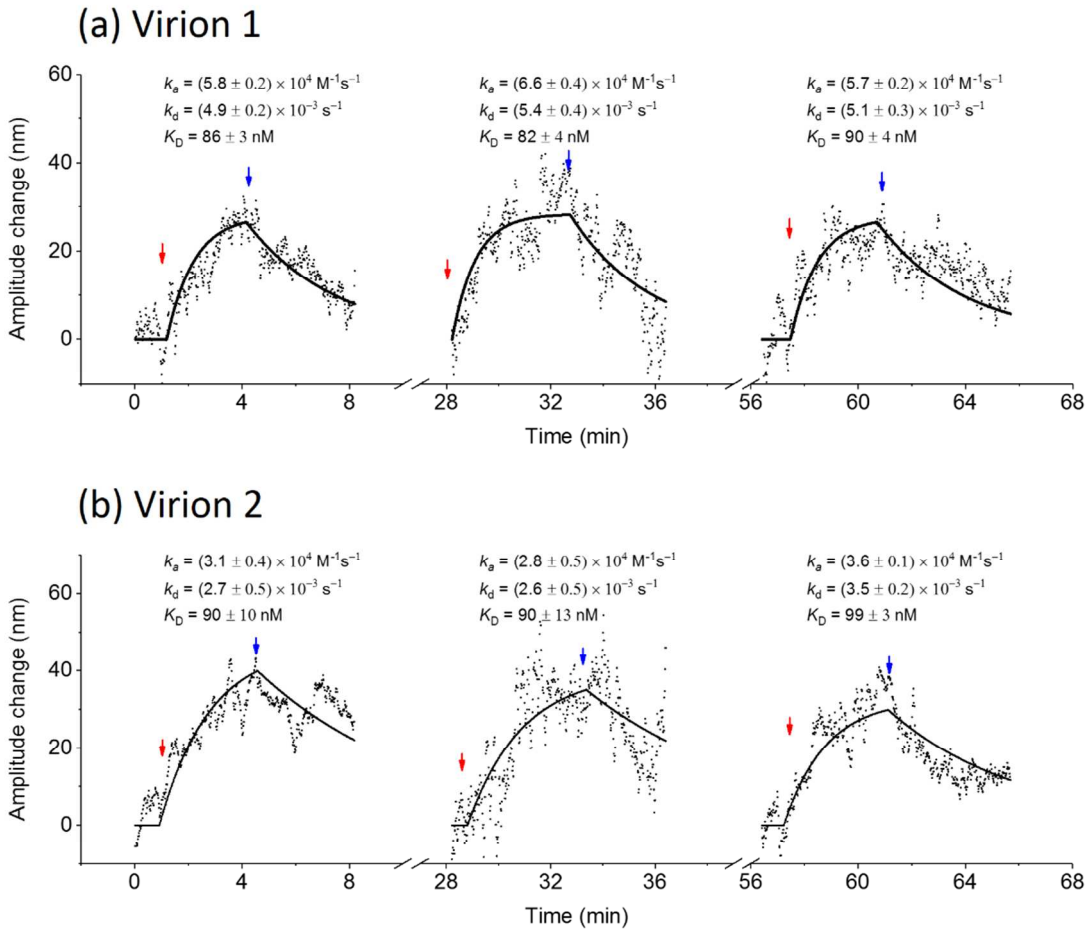

Figure S8. Evaluation of the reliability of virion oscillation measurement. (a) GPR55 – Tocrifluor binding was measured three times for the virion (virion 1), where the red and blue arrows mark the starting points of the association phase and dissociation phase in each measurement. Note that the dissociation was performed for 24 minutes to allow complete dissociation but was recorded for only 4 minutes. k_a, k_d, and K_D were determined in each repeated measurement, and variability is less than 10%. (b) Another virion (virion 2) recorded simultaneously with virion 1 shows similar binding kinetic constants. The concentration of Tocrifluor: 200 nM. Applied voltage: Amplitude = 0.4 V and frequency = 5 Hz. Buffer: 40 times diluted PBS (4 mM) with pH = 7.4.

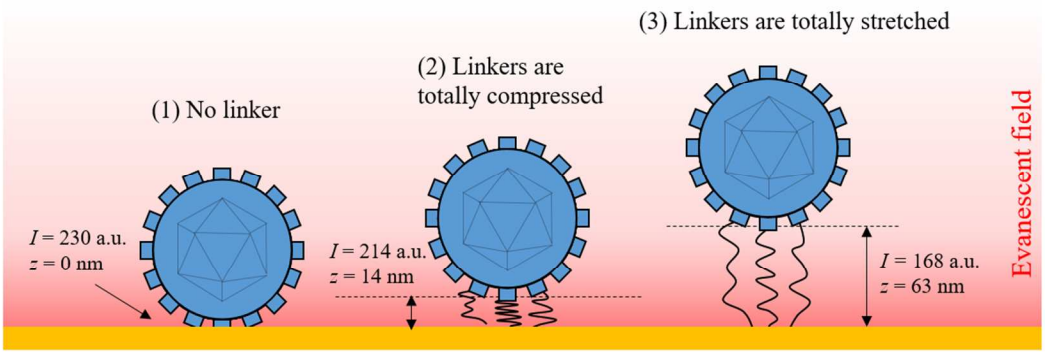

Figure S9. Model illustration of the virion oscillation. (1) A virion directly attached to the gold chip without PEG linkers, wherein the virion-gold chip distance *z* is 0 and the plasmonic imaging intensity *I* is 230 a.u. (2) PEG linkers are compressed, wherein *z* is determined by the Flory radius of the PEG, which is ~14 nm. Compared with (1), *I* decreases due to the decay of the evanescent field, and is calculated to be 214 a.u. using Eq.2. (3) PEG linkers are totally stretched, wherein *z* reflects the length of the PEG, which is 63 nm. *I* is decreased to 168 a.u..

1. Binding experiment is performed and the oscillation is recorded.

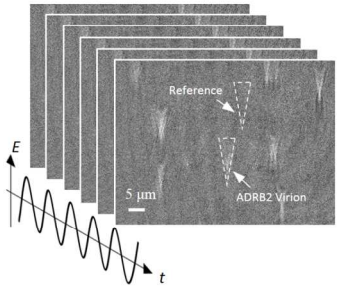

2. The intensity of a virion region (I_v) and a reference region (I_r) are measured.

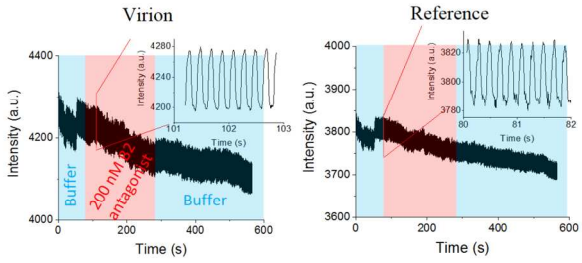

3. The oscillation signal (I) of the virion is obtained by $I = I_v - I_r$.

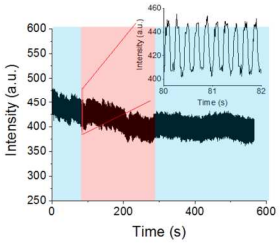

4. The maximum intensity in each cycle are aligned to the same level (the intensity at z = 14 nm).

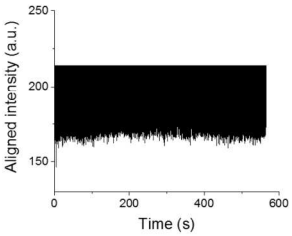

5. Convert intensity to virion-gold chip distance.

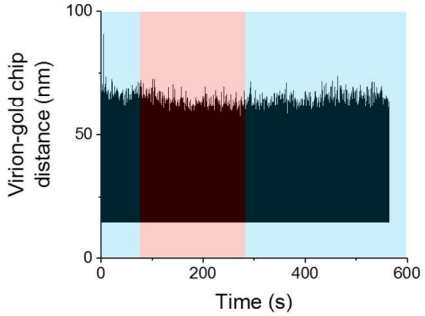

6. Obtain the oscillation amplitude in every one second using FFT.

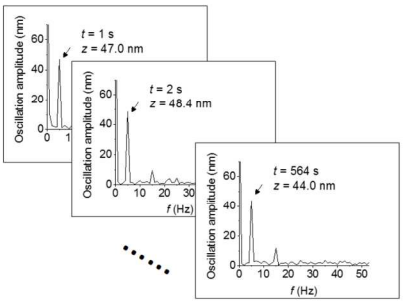

7. Plot oscillation amplitude vs. time.

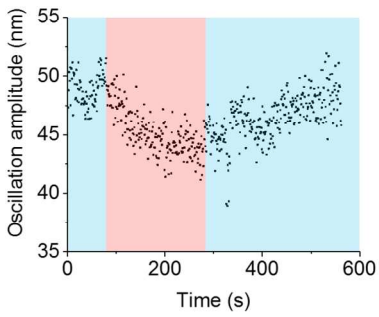

8. The initial oscillation amplitude is set as the baseline, and the y axis is re-expressed as oscillation amplitude change. The curve is fitted with first order kinetics model.

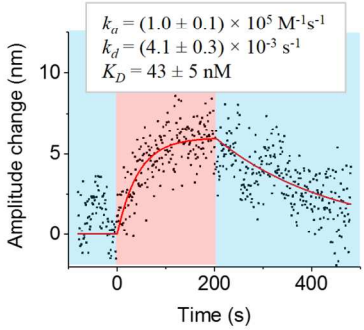

Figure S10. Data processing of D1 antagonist – DRD1 binding experiment. The concentration of D1 antagonist is 200 nM. Applied voltage: Amplitude = 0.4 V and frequency = 5 Hz. Buffer: 40 times diluted PBS (4 mM) with pH = 7.4.

References

1. Dalton, J.A., Lans, I. & Giraldo, J. Quantifying conformational changes in GPCRs: glimpse of a common functional mechanism. *BMC Bioinformatics* **16**, 124 (2015).
2. Ozalp, V.C. Acoustic quantification of ATP using a quartz crystal microbalance with dissipation. *Analyst* **136**, 5046-5050 (2011).
3. Hatty, C.R. et al. Investigating the interactions of the 18 kDa translocator protein and its ligand PK11195 in planar lipid bilayers. *Biochimica et Biophysica Acta (BBA) - Biomembranes* **1838**, 1019-1030 (2014).
4. Osypova, A. et al. Sensor Based on Aptamer Folding to Detect Low-Molecular Weight Analytes. *Analytical Chemistry* **87**, 7566-7574 (2015).
5. Patel, A.R., Kanazawa, K.K. & Frank, C.W. Antibody Binding to a Tethered Vesicle Assembly Using QCM-D. *Analytical Chemistry* **81**, 6021-6029 (2009).
6. Peh, W.Y.X., Reimhult, E., Teh, H.F., Thomsen, J.S. & Su, X. Understanding Ligand Binding Effects on the Conformation of Estrogen Receptor α-DNA Complexes: A Combinational Quartz Crystal Microbalance with Dissipation and Surface Plasmon Resonance Study. *Biophysical Journal* **92**, 4415-4423 (2007).
7. Carta, G. & Jungbauer, A. Protein chromatography: process development and scale-up. (John Wiley & Sons, 2010).
8. Wang, S. et al. Label-free imaging, detection, and mass measurement of single viruses by surface plasmon resonance. *Proceedings of the National Academy of Sciences* **107**, 16028-16032 (2010).
9. Mettenleiter, T.C. Herpesvirus Assembly and Egress. *Journal of Virology* **76**, 1537-1547 (2002).
10. Hu, Y. et al. Study of fibrinogen adsorption on poly(ethylene glycol)-modified surfaces using a quartz crystal microbalance with dissipation and a dual polarization interferometry. *RSC Advances* **4**, 7716-7724 (2014).
11. Fu, W. et al. Dopamine D1 receptor agonist and D2 receptor antagonist effects of the natural product (-)-stepholidine: molecular modeling and dynamics simulations. *Biophys J* **93**, 1431-1441 (2007).